# Charge carrier properties in P-type layers of silicon on sapphire

M. Roux, D. Bielle-Daspet

Classification
*Physics Abstracts*
07.50 — 72.40

# Charge carrier properties in P-type layers of silicon on sapphire (*)

M. Roux and D. Bielle-Daspet

Centre d'Etude Spatiale des Rayonnements (**), 9, avenue du Colonel-Roche, BP 4346, 31029 Toulouse, France

(*Reçu le 27 février 1981, révisé le 22 mai 1981, accepté le 29 mai 1981*)

**Résumé.** — Densité et mobilité des trous à l'équilibre et propriétés des porteurs créés par photoexcitation sont étudiées par des mesures de Hall et les photoréponses transitoires à une excitation par laser pulsé (durée de 30 ns à mi-hauteur) de longueur d'onde 1,06 et 0,53 μm. Les réponses transitoires concernent à la fois les photocourants de diffusion dus aux trous ou électrons libres et la photoconductivité à courant constant liée aux variations de densités et/ou mobilités des porteurs de charge. Les résultats portent sur des couches épitaxiales d'épaisseur 0,9 à 2,4 μm et de résistivité 0,7 à 2,0 Ω.cm, étudiées dans le domaine de température 300-50 K et pour des impulsions lumineuses d'énergie $10^{-4}$ à $10^{2}$ mJ.
Les mesures transitoires montrent l'existence de zones isolantes (niveau de Fermi interne $E_{Fj} \sim E_V + 0{,}32$ eV) associées à un fort effet de pièges à électrons $E_t \sim E_C - 0{,}17$ eV. Les zones isolantes paraissent réparties dans le volume des couches et sont responsables d'une diminution de 33 % de la conductivité de ces couches, à température ambiante. Ceci se compare favorablement à la compensation par niveaux donneurs et aux effets de dislocations obtenus à partir des données de Hall.

**Abstract.** — Equilibrium hole density and mobility and photoexcited carrier properties are studied using Hall measurements and transient photoresponses to pulsed laser beam (30 ns half-width duration) of 1.06 and 0.53 μm wavelength. The transient responses involve both the diffusion photocurrents due to free excess holes or electrons and the photoconductivity under constant current due to the variations induced in the charge carrier densities and/or mobilities. Results deal with 0.9 to 2.4 μm thick epitaxial layers of 0.7 to 2.0 Ω.cm resistivity which are studied in the temperature range 300-50 K and for $10^{-4}$ to $10^{2}$ mJ.cm$^{-2}$ incident light pulse energy.
From transient measurements the existence of insulating zones (internal Fermi level $E_{Fj} \sim E_V + 0.32$ eV) associated with electron traps $E_t \simeq E_C - 0.17$ eV is deduced. The insulating zones should spread out in the layer volume and are responsible for a 33 % decrease in the layer conductivity at room temperature. This is compared with donor-type compensation and dislocation effects obtained from the Hall data.

1. **Introduction.** — In integrated circuits, the electrical quality of the S.O.S. layers plays a fundamental role. This quality, however, remains difficult to control, especially because of the great density of structural defects (dislocations, twins, precipitates) present in these layers [1, 2, 3]. The purpose of this paper is to define the electrical quality of epitaxial layers of S.O.S. by means of a correlated study of mobilities, densities, and capture processes of the charge carriers. This study uses both the usual Hall effect data and the transient electrical photoresponses to an excitation by a pulsed laser beam (wavelengths 1.06 μm and 0.53 μm). The photoresponses used are those related to the excesses of majority and minority carriers and to the photoconduction processes. It uses the results of previous research on bulk silicon [4] and polycrystalline silicon [5, 6].

In previous work, the comparison between diffusion current and conductivity transient photoresponses was shown to allow a differentiation between the contributions of free carriers and trapping phenomena. Where recombination, trapping, and compensation phenomena associated with defects are concerned (including donor- and acceptor-like defects), this comparison also brings out the influence i) associated with the level of induced excess carriers, and ii) associated with zones of electrical in-homogeneity such as *Potential barriers* surrounding extended *defects* which exist in materials of low cristalline quality.

The samples studied are Boron-doped epitaxial layers with resistivities of the order of 1 Ω.cm, thicknesses 0.9 μm, 1.3 μm or 2.4 μm, manufactured

(*) Work supported by the Groupement Circuits Intégrés au Silicium (G.C.I.S.) program (Convention AO 1896 issue de AO 1825).

(**) Laboratoire propre du CNRS, conventionné avec l'Université Paul-Sabatier.

by the L.E.T.I. ([1]). These samples and the experimental conditions, particularly the use of the pulsed laser at 1.06 μm and 0.53 μm wavelength and the measurements in the 300 K-50 K temperature range, are described in section 2.

Section 3 presents the obtained results. The first part of section 3 is devoted to the D. C. measurements of the resistivity $\rho$, the carrier density $p_H$, and mobility $\mu_H$. These studies of the conduction of the samples were done not only to determine the electrical characteristics of the samples, but also to have a reference point for the transient studies. The latter focus on the amplitude and form of the rise and fall of the photoresponses of diffusion current ($i_n(t)$ due to minority carriers and $i_p(t)$ due to majority carriers) and of conductivity $\Delta V_\sigma(t)$ as a function of the pulse exciting energy $E_0$, the wavelength $\lambda$, and the temperature $T$.

A discussion of these results appears in section 4.

2. **Experimental conditions.** — The studies involved three groups of 5 × 25 mm² samples of boron doped P-type silicon (elaborated on $Al_2O_3$ substrate of ~ 0.35 mm thickness), Hall bar shaped and with thicknesses $w$ = 0.9 μm, 1.3 μm and 2.4 μm (Fig. 1). Each epitaxial layer sample has six implanted contacts : five $PP^+$ ohmic contacts, and one $PN^+$ injecting contact (except on the thinnest sample $w$ = 0.9 μm, where all the contacts were $PP^+$ type). The purpose of the $PN^+$ contact is to allow a study of the diffusion photocurrents associated with excess minority carriers (see section 3.2).

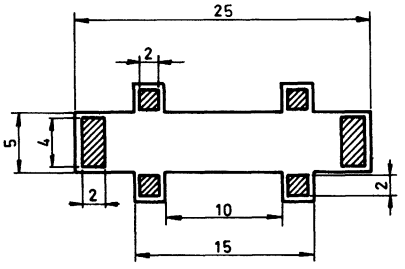


Fig. 1. — Sketch of the samples studied (dimensions in mm).

Hall data are obtained for a magnetic field of 2 500 gauss and a polarization current of 100 μA in a temperature range 300 K-50 K.

The laser apparatus used to study the photoresponses has been described earlier [7] : it includes two neodymium doped glass bar pulsed lasers ($\lambda$ = 1.06 μm, triangular pulse of total length $\delta$ = 60 ns, nominal energy $E_0 \leqslant$ 1 to 3 J), associated with an electrooptical cell (rectangular pulse adjustable to 2, 6 or 15 ns) and a frequency multiplier ($\lambda$ = 0.53 μm). The signals are treated using a Tektronix WP2221 transient digital analyzer with a PDP 11 computer, and the temperature tests are done in a regulated He cryostat equipped with 3 optical windows.

The absorption coefficients in the silicon for the wavelengths used are $\alpha \gtrsim 40$ cm$^{-1}$ at $\lambda$ = 1.06 μm and $\alpha = 8 \times 10^3$ cm$^{-1}$ at $\lambda$ = 0.53 μm. The use of these two wavelengths allows the average penetration depth $l = 1/\alpha$ to be varied from $l \sim 250$ μm $\gg w$ for $\lambda$ = 1.06 μm, to $l \sim 1.25$ μm $\lesssim w$ ar $\lambda$ = 0.53 μm. This therefore in turn allows to obtain the relative influences of the layer surface and the $Si/Al_2O_3$ interface, for the photoresponse measurements. However, the photoexcitation measurements still have the problem of the effective illuminated surface area, i.e., of the optical masking of the samples. In particular, during the experiments using laser illumination at $\lambda$ = 1.06 μm, multiple reflections of the beam may occur at the $Si/Al_2O_3$ interface and especially in the $Al_2O_3$ substrate. Therefore, a study of the energy $E$ transmitted by the silicon-substrate structure was done, as a function of the distance $x$ to the illuminated area. (For these measurements, a 0.5 mm diameter detector was used and the incident illumination $E_0$ was limited to a 1 mm slit located at the centre of the epitaxial layer sample, Fig. 2.) Although the trans-

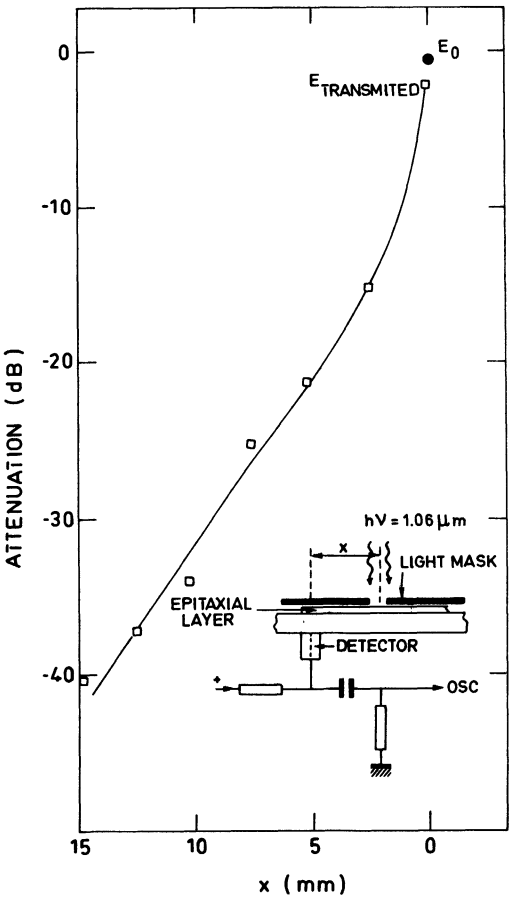


Fig. 2. — Study of the luminous energy transmitted by the $Si$-$Al_2O_3$ ensemble : 1.06 μm laser pulse, incident illumination limited to a 1 mm slit. Variation of the energy transmitted as a function of the distance $x$ to the illuminated slit.

([1]) Laboratoire d'Electronique et de Technologie de l'Informatique, Grenoble, France.

mitted intensity falls rapidly as a function of $x$ (see Fig. 2), the results show that a residual illumination remains at the level of the contacts, which corresponds to a 25 dB attenuation with respect to the incident energy $E_0$.

3. **Experimental results.** — 3.1 CONDUCTION PROPERTY IN STATIONARY REGIME. — The values of $\rho$, $\mu_H$ and $P_H$ measured at ambient temperature and as a function of temperature from $T = 300$ K to 50 K are given in table I and figures 3 to 5.

Table I. — *Values of $\rho$, $P_H$ and $\mu_H$ measured at ambient temperature.*

| | Sample | | |
|---|---|---|---|
| 300 K values | $W = 0.9$ μm | $W = 1.3$ μm | $W = 2.4$ μm |
| $\rho$ (Ω.cm) | 0.7 | 1.6 | 2.0 |
| $P_H$ (cm$^{-3}$) | $5 \times 10^{16}$ | $7.5 \times 10^{16}$ | $3.6 \times 10^{16}$ |
| $\mu_H$ (cm$^2$/V.s) | 90 | 50 | 80 |

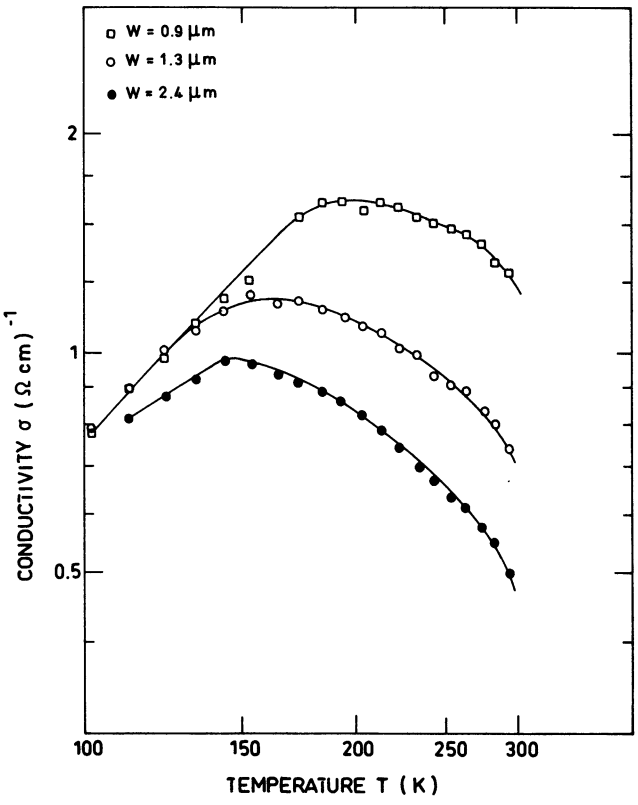


Fig. 3. — Variation of equilibrium conductivity $\sigma$ with temperature $T$.

Generally, these results show that, for the temperature range considered, the mobilities $\mu_H$ remain small compared to the values which would be found for bulk silicon of the same resistivity : the $\mu_H(T)$ values remain lower than $10^2$ cm$^2$.V$^{-1}$.s$^{-1}$ for the entire temperature range and for the three epitaxial layer groups studied (Fig. 4). At the same time, the densities measured $P_H \leqslant 7.5 \times 10^{16}$ cm$^{-3}$ are large with respect to the values which would be

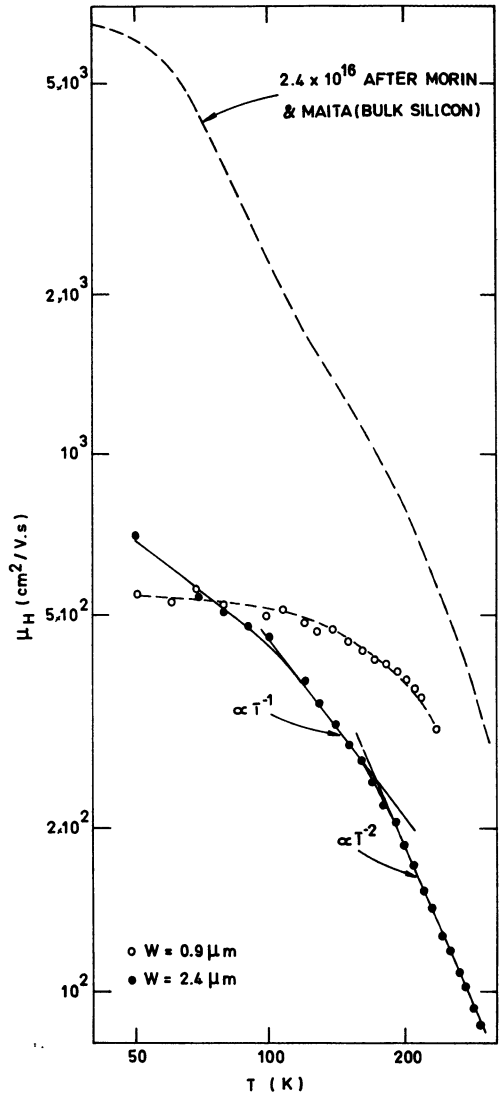


Fig. 4. — Hall mobility $\mu_H$ *vs.* temperature $T$ (magnetic field 2 500 Gauss). Comparison with P-type, boron doped ($2.4 \times 10^{16}$ cm$^{-3}$) bulk silicon data from Morin and Maita [20].

found in a monocrystal of the same resistivity ($p_{mono} \leqslant 2 \times 10^{16}$ cm$^{-3}$).

At the lowest temperatures $T < 70$ K the carrier density $p_H(T)$ (Fig. 5) indicates an activation energy $E_A - E_V = 0.045$ eV for the acceptor level [8] which is in agreement with the boron level. But at the highest temperatures (70 K $< T <$ 300 K) the density $p_H$ increases monotonically with $T$ : this type of behaviour has also been observed in S.O.S. films by other authors [9, 10] and would seem to indicate the presence of donor-type compensation levels.

As far as the mobility $\mu_H$ is concerned, its evolution with temperature $\mu_H(T)$ varies from sample to sample (Fig. 4). In particular, i) for the thickest sample $w = 2.4$ μm, three regions can be defined : at temperatures above 200 K, the variation of the mobility is of the form $\mu_H \propto T^{-2}$; at lower temperatures $T < 100$ K the mobility increases only weakly as the temperature decreases; at intermediate temperatures

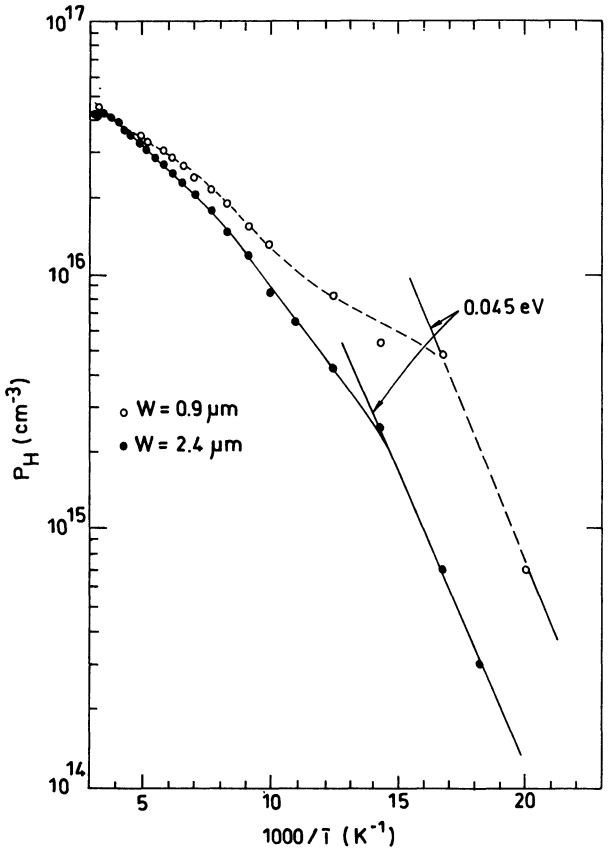


Fig. 5. — Hole density $P_H$ *versus* reverse temperature $1/T$.

200 K > $T$ > 100 K the mobility has the form $\mu_H \propto T^{-1}$ (see Fig. 4); ii) for the thinnest sample $w$ = 0.9 µm, on the other hand, the mobility changes little as a function of temperature over the entire range $T \leqslant$ 200 K.

In order to compare these results with those for bulk silicon, we will use a general expression for the mobility of the form :

$$\mu^{-1} \sim \mu_l^{-1} + \mu_{ion}^{-1} + \mu_{neut}^{-1} + \mu_d^{-1} \qquad (1)$$

where

$\mu_l \propto T^{-2.7}$ (lattice scattering effect on holes in P-type silicon [11])
$\mu_{ion} \propto T^{3/2}$ (ionized impurities)
$\mu_{neut} \propto T^0$ (neutral impurities)
$\mu_d \propto T^1$ (dislocations).

The variation $\mu_H(T)$ observed for the samples therefore indicate that the influence of ionized impurities and dislocations on the mobility $\mu_H$ is much greater on thin samples than on thick samples. Indeed, for the thinnest sample, lattice scattering appears to rule out the hole mobility $\mu_H(T)$ only at temperature near the room temperature : scattering by ionized impurities (which dominates in the lowest temperature range) alone cannot explain such a behaviour. Significant effect $\mu_d(T)$ of dislocations is thus necessary to explain the measured $\mu_H(T)$ variations. This is in agreement with results obtained in reference [12] which also show that the density of crystalline defects (dislocation or twins) decreases as the distance from the $Si/Al_2O_3$ interface increases, i.e., the density of these defects must be higher in the thinnest sample $w$ = 0.9 µm.

3.2 TRANSIENT PHOTORESPONSE RESULTS. — The transient photocurrents studied are the short circuit currents $i(t)$ between contacts C(PP$^+$) and B(PN$^+$), or between C(PP$^+$) and A(PP$^+$), when the incident illumination is limited either to contact B(PN$^+$) ($i(t) = i_n(t)$) or to contact A(PP$^+$) ($i(t) = i_p(t)$) (see fig. 6*a*). The direction of the signals observed corresponds to the collection :

— of electrons, minority carriers in the layers, for the currents $i_n(t)$ associated with the N$^+$/SiP contacts,

— of holes, majority carriers in the layers, for the currents $i_p(t)$ associated with the contacts P$^+$/SiP.

The photoconductivity signals are the variations of potential received at the contacts of the sample polarized at constant current $I_0$ = 100 µA and subjected to laser illumination on 1 mm slit at the centre (see Fig. 6*b*). The signals observed always correspond

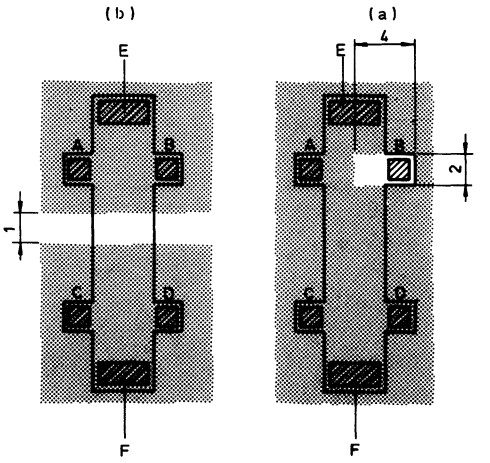


Fig. 6. — Optical masks used for the laser illumination studies : *a*) photocurrent studies, *b*) photoconductivity studies.

to an increase in conductivity for the sample. However, for illumination at $\lambda$ = 1.06 µm (see section 2, Fig. 2), the effects of multiple reflections $E(x)$ on the incident beam $E_0$ give rise to a parasite signal. This signal corresponds to a voltage component $V$ :

i) whose influence on the observed signals appears only for the most intense excitation $E_0$ ;

ii) which is independent of the value of the polarization current $I_0$, both in amplitude and form ;

iii) which affects mainly the rise of the signal;

iv) whose amplitude and direction vary with the sample studied for a given $E_0$ ;

v) which is absent for $\lambda$ = 0.53 µm (high absorption coefficient in silicon).

This parasitic voltage $V$ is therefore in agreement with the sum of the open circuit photovoltage res-

ponses generated — due to the configuration of the photoconductivity $\Delta V$ measurement circuit — by multiple reflections $E$ (1.06 μm) at the extreme contacts E and F of the sample : $V(t) = \sum v_{oc}(t) = v_{oc1} - v_{oc2}$. In the present measurements the magnitude of $V$ is then due to the polarization current $I_0$ whose effect is to favour the photovoltage component $v_{coF}$ of the reverse biased contact F [7]. In the following results, only the photoconductivity signal $\Delta V_\sigma(t) \propto I_0$ will thus be considered. We note that, by comparison, the contribution of the illumination $E(x)/E_0$ at 1.06 μm is less easy to distinguish in the short-circuit photocurrent responses. In fact, a component related to the masked contact ($i_C(t)$ for masked contact C, see Fig. 6*a*) is superposed on the component due to the illuminated contact. The $i_C(t)$ component is added to the component $i_{nB}(t)$ (for the case where the $N^+$ contact is illuminated) or substracted from the $i_{pA}(t)$ component (for the case where the $P^+$ contact is illuminated). In this case, we thus have a contribution of parasitic current which has a comparable dependence in function of energy as the original signal. On the contrary, the evolution of the amplitude $V$ of the parasitic photovoltage is more rapid as a function of energy than that of the measured photoconductivity signal $\Delta V_\sigma(t, I_0 \neq 0)$ on which it is superposed : it only appears for strong injection and is therefore easily distinguished from the original signal $\Delta V_\sigma(t)$.

3.2.1 *Comparative forms of the various photoresponses.* — The general forms of the photoresponses $i(t)$ and $\Delta V_\sigma(t)$ are the same at 1.06 μm and 0.53 μm. These two types of photoresponses, which correspond respectively to free electrons or holes (photocurrent $i_{n,p}(t)$) and to the variation in the conductivity induced in the material, may be related to diverse phenomena (see [4]). They are compared in figure 7.

These forms reveal some typical features which may be summarized as follows :

i) whatever the photoresponses, two types of components are observed, one fast and the other slow, but they have different relative amplitudes according to the exact response ;

ii) the short circuit photocurrent $i(t)$ response appears as the sum of a fast component $i_1(t < \delta)$ which occurs during the excitation pulse and has a direction corresponding to the collected carriers, and a slow component $i_2(t)$ which extends over several μs. The fast component $i_1(t < \delta)$ demonstrates that the free carrier lifetime $\tau$ in the layers is small compared to the length $\delta \sim$ 30-60 ns of the exciting pulse. The slow component is identical for the two types of carriers (negative in both cases, and of comparable duration) and therefore cannot be attributed to a carrier diffusion response ;

iii) the photoconductivity signals $\Delta V_\sigma(t)$ appear to have a form which is typical in the whole exciting energy ranges $E_0$ used (Fig. 8) and is completely identical for the two wavelengths 0.53 μm and 1.06 μm

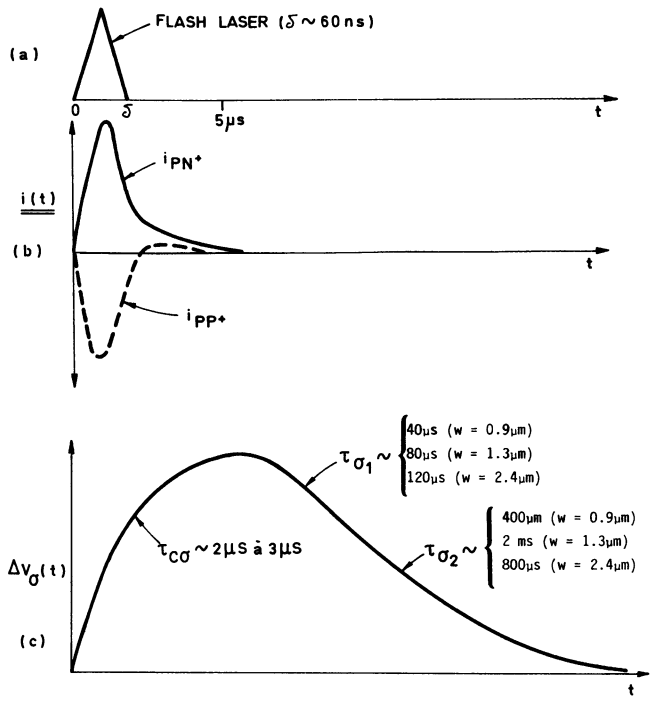


Fig. 7. — Forms of the observed transient photoresponses : *a*) exciting light pulses, *b*) short circuit photocurrent responses $i(t)$, measured for $\lambda = 1.06$ μm, *c*) transient photoconductivity responses $\Delta V_\sigma(t)$ measured for $\lambda = 0.53$ and $\lambda = 1.06$ μm.

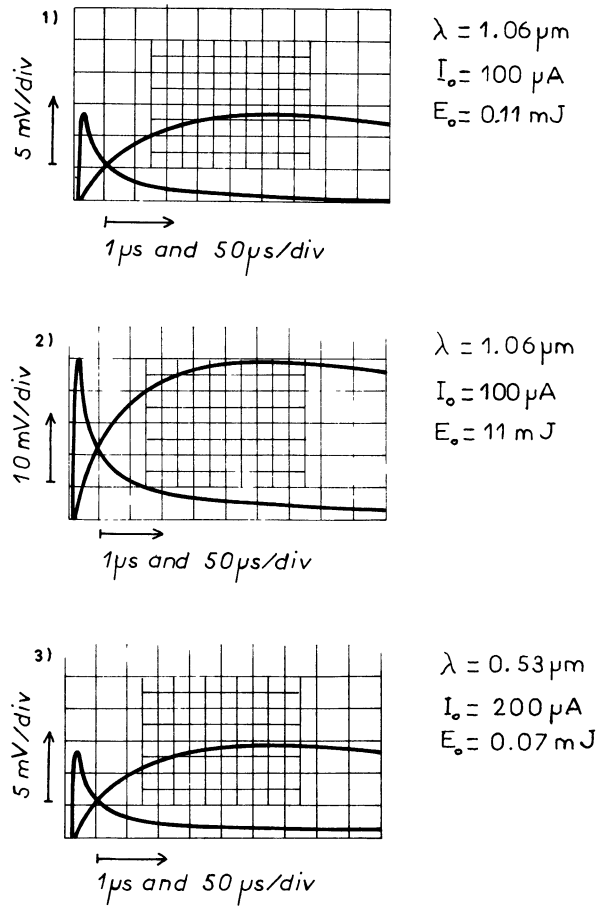


Fig. 8. — Transient photoconductivity signals observed at various exciting pulse energy $E_0$ (1, 2) and wavelength $\lambda$ (1, 3).

of the excitation pulses. First, they are characterized by a slow and exponential rise with time constant $\tau_{c\sigma}$ of the order of 2 to 3 μs depending upon the sample. We note, moreover, that the maximum of the signal corresponds to the end of the signal $i(t)$ (maximum for $t \sim$ several μs $\gg \delta$). Second, their decay cannot be described by a simple exponential. It has an instantaneous time constant $\tau_\sigma(t)$ which increases with time. It will simply be described here by its initial time constant $\tau_{\sigma 1}$ and its final time constant $\tau_{\sigma 2}$, measured respectively at the start and trailing edge of the decay. The values of $\tau_{\sigma 1}$ and $\tau_{\sigma 2}$ are given in figure 7 ; note that they are large. This is therefore not the response of a homogeneous material such as bulk silicon, in which the lifetime of free carriers may be measured from the photoconductivity decay, at least in the low to mean carrier injection range [4, 13, 14].

3.2.2 *Evolution as a function of the injection energy* $E_0$. — In figures 9*a* and 9*b*, the evolution of the short-circuit photoresponses maximum $i_{max}$ is shown as a function of incident energy $E_0$ ($\lambda = 1.06$ μm). Whether for signals generated by illumination of a $P^+$ contact (majority holes collected) or of a $N^+$ contact (minority electrons collected), the value of $i_{max}$ is not proportional to $E_0$ but rather less than proportional.

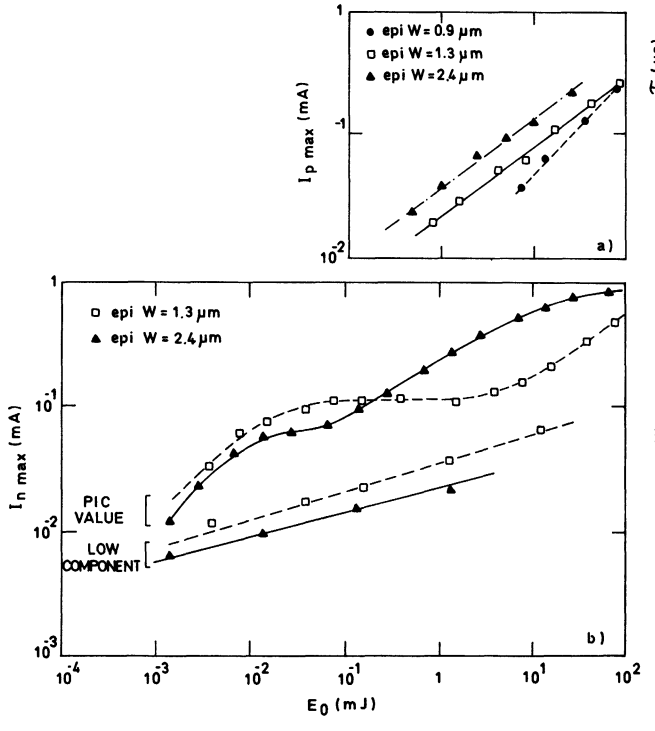


Fig. 9. — Variation with the excitation intensity $E_0$ ($\lambda = 1.06$ μm) of the short circuit photocurrent amplitude observed (see Fig. 6) by illumination : *a*) on a $P^+$ lateral contact ($I_{pmax}$) ; *b*) on the $N^+$ contact (Pic value $I_{nmax}$ and low component amplitude $i_n(t = \delta)$).

For $i_{pmax}(E_0)$ due to majority carriers (Fig. 9*a*) the saturation value $i_{sat} = V_D/Z_{tot}$ imposed by the measurement circuit — $V_D$ diffusion potential of the lighted contact — is never reached. On the other hand, for minority carriers (Fig. 9*b*) a flatness in the curve is observed (see Table II) in the $i_{nmax}(E_0)$ curves which agrees with the value of $i_{sat}$. But the value of $i_{nmax}$ continues to smoothly increase with $E_0$ in the highest injection energy range. This may be explained by the effect of high injection : the total impedance $Z_{tot}$ of the sample between the contacts used decreases with the increase of $E_0$ because a large part of the sample is illuminated either directly with the incident beam of energy $E_0$ or by multiple reflections $E(x)$. The increase in conductivity which results from the creation of electron-hole pairs in the sample decreases $Z_{tot}$ so that an increase of the maximum value of the current $i_{sat} = V_D/Z_{tot}(E_0)$ is observed (where $V_D$ is the barrier height of the contact considered ; $V_D$ for the contact is deduced by the maximum amplitude of the open circuit saturation signal $V_{ocsat}$ [13]).

The transient photoconductivity results are given in figures 10*a* and 10*b*. A saturation of the signal maximum $\Delta V_{\sigma max}$ appears for incident energies $E_0 \sim 10^{-3}$ mJ, but never reaches the limiting value ([2])

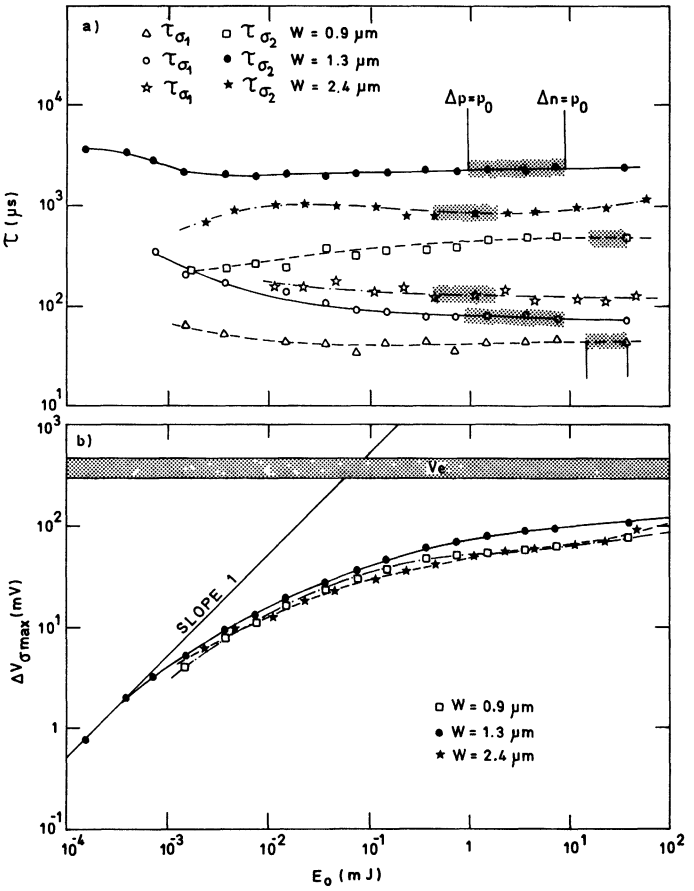


Fig. 10. — Variation with the excitation intensity $E_0$ ($\lambda = 1.06$ μm) of the photoconductivity signal : *a*) decay time constant at the decay beginning $\tau_{\sigma 1}$ and latter part $\tau_{\sigma 2}$, *b*) amplitude $\Delta V_{\sigma max}$.

([2]) The value of $V_e$ corresponding to the layer unmasked portion only represent a lower limit to the maximum amplitude of the photoconductivity signal $\Delta V_{\sigma sat}$ since multiple reflections inject 50 % more radiation into either side of the illuminated zone. The value of $V_e$ used to determine $\Delta V_{\sigma sat}/V_e$ in table II is weighted by this factor of 50 %.

Table II.

| Sample / 1.06 μm response | $w = 0.9$ μm | $w = 1.3$ μm | $w = 2.4$ μm |
|---|---|---|---|
| $i_{sat}$ ($N^+$ contact) | — | $1.15 \times 10^{-1}$ mA | $6.5 \times 10^{-2}$ mA |
| $\Delta V_{\sigma sat}$ | 70 mV | 100 mV | 90 mV |
| $\Delta V_{\sigma sat}/V_e$ | 1/4 | 1/3 | ~ 1/3 |

$V_e$ (Table II) which corresponds to an infinite value of the conductivity in the layer illuminated zone. It can also be noted that the decay time constants $\tau_{\sigma 1,2}$ are not much influenced by $E_0$ in the $E_0 > 10^{-3}$ mJ range. Such a behaviour is characteristic of the onset of a high injection phenomenon at the highest incident energies $E_0 > 10^{-3}$ mJ ($\lambda = 1.06$ μm).

3.2.3 *Behaviour of the photoconductivity decay as a function of temperature.* — It can be seen from figures 11 and 12 that, when the temperature decreases from 300 K to 100 K, the values of the decay time constants $\tau_{\sigma 1,2}$ first increase, then stabilize at low

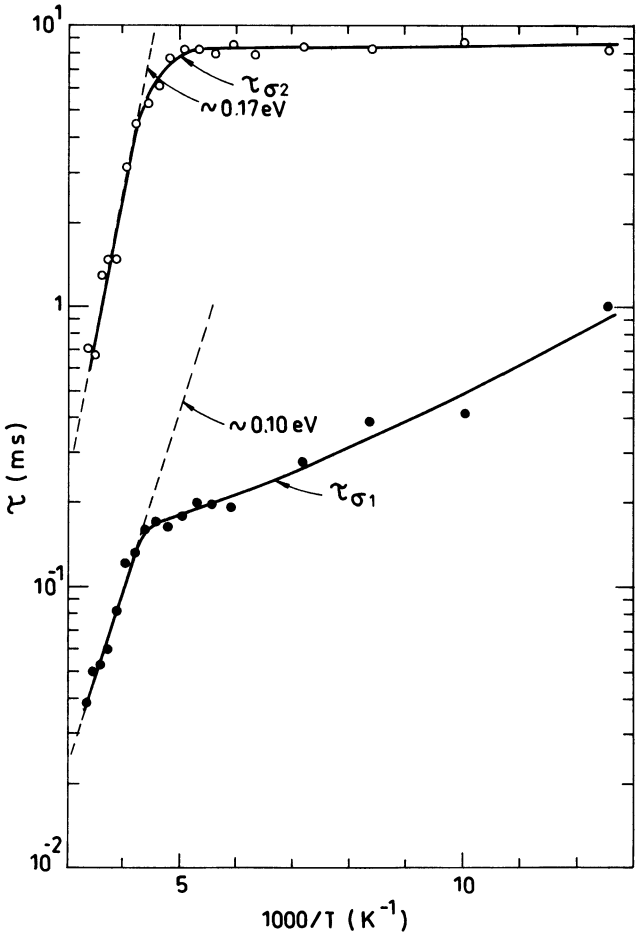


Fig. 11. — Variation with measurement temperature of the photoconductivity response decay time constants $\tau_{\sigma 1,2}$ : sample with layer thickness $w = 0.9$ μm; beam pulse $E_0 = 0.35$ mJ, $\lambda = 1.06$ μm.

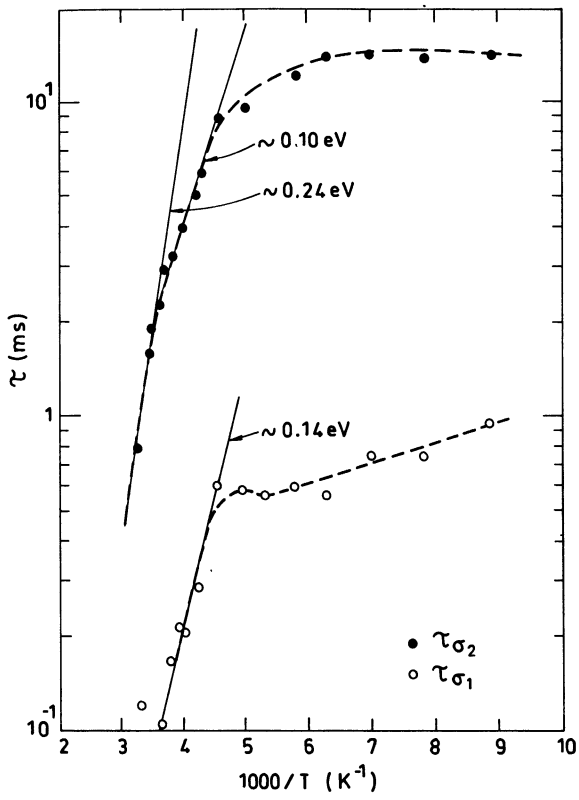


Fig. 12. — *Id.* as figure 11 : sample with layer thickness $w = 2.4$ μm ; beam pulse $E_0 = 0.22$ mJ, $\lambda = 1.06$ μm.

temperatures $T < 200$ K. This behaviour is characteristic of the re-emission of trapped carriers. From the slope of the $\tau(1/T)$ semilogarithmic plot — $T \gtrsim 250$ K range —, the values $E_{1,2}$ of the trapping energy levels estimated from a band edge are the following :

$$E_c - E_t \quad \text{or} \quad E_t - E_v = \\ = k(\text{d Ln}(\tau)/\text{d}(1/T)) - 3/2\, kT$$

epitaxial layer $w = 0.9$ μm :

$$E_1 = 0.10 \text{ eV},$$

$$E_2 = 17 \text{ eV} \Rightarrow \langle E_t \rangle\ 0.14 \text{ eV} \pm 0.03 \text{ eV}$$

epitaxial layer $w = 2.4$ μm :

$$E_1 = 0.14 \text{ eV},$$

$$E_2 = 0.10 \text{ to } 0.24 \text{ eV}$$

$$\Rightarrow \underline{\langle E_t \rangle\ 0.17\ \text{eV} \pm 0.07\ \text{eV}}\ .$$

4. **Discussion of the results.** — The experimental results presented above lead to the following preliminary observations.

1) From the Hall measurement results, we have found a strong influence due to ionized impurities and dislocations which is consistent with a limitation due to zones of cristalline in-homogeneity. Particularly the small values measured for the mobility (see Section 3.1 and Fig. 4) compared with the values for bulk silicon may be interpreted as a limitation related to these zones of in-homogeneity.

2) Transient photoresponses are not signals which allow the usual interpretation leading to a measurement of the lifetime of free carriers. Indeed, the diffusion electron and hole components $i_{n,p}(t)$ of the measured short-circuit current responses follow the excitation signal and thus show that the lifetime of free carriers is, in the S.O.S. layers studied very small compared with the exciting pulse duration $\delta = 60$ ns. On the other hand the photoconductivity responses $\Delta V_\sigma(t)$ demonstrate that trapping phenomena in the material are very important.

After evaluating the free carrier injection levels $\Delta n, p$ used, we will consider in the following section the types of phenomena which must be invoked to explain the transient photoresponses, which in turn will permit us to analyse these results.

4.1 ESTIMATE OF THE DENSITY $\Delta n, p$ OF THE EXCITED CARRIERS. — The lifetimes $\tau_{n,p}$ of the free carriers are very small in the silicon layers studied compared to the total duration of the laser pulse $\delta = 60$ ns and we therefore have a pseudo-continuous regime of injection of free carriers during the time $\delta$. The densities $\Delta n, p$ of free carriers created in the material by laser excitation will then be of the form $\Delta n, p = G.\tau_{n,p}$ where $G$ is the average value of carrier generation rate of the light pulse used.

In the above free carrier lifetime $\tau_{n,p}$, both the loss rate of carriers $(1/\tau_G)$ — due to the losses near the silicon surface and Si-$Al_2O_3$ interface — and the bulk recombination rate $(1/\tau_V)$ are included. The free carrier lifetime

$$\tau_{n,p} = (1/\tau_V + 1/\tau_{Gn,p})^{-1} \qquad (2)$$

is thus at most equal to the carrier loss component $\tau_G$. As it is well known that the recombination velocity $s_1$ near the Si-$Al_2O_3$ interface is very strong, the $\tau_G$ values in our measurements then satisfy the condition [13, 15] :

$$w^2/\pi^2\, D_{n,p} \leqslant \tau_{Gn,p} \leqslant 4\, w^2/\pi^2\, D_{n,p} \qquad (3)$$

where the lower and the upper limits correspond to the infinite and nul recombination velocities $s_2$ at the silicon surface, respectively (i.e., $s_2 \gg 2\, D/w$ and $s_2 \ll 2\, D/w$). Notice that the $s_2$ value at the Si-$SiO_2$ surface may be low enough [16] for the condition $s_2 \ll 2\, D/w$ of a low recombination velocity to be satisfied in the layers studied. From relations (2) and (3), we shall estimate the order of magnitude of the induced excess carrier densities $\Delta n, p$ by using for $\tau_{n,p}$ the lowest calculated values of the carrier loss component $\tau_G = w^2/\pi^2\, D$. We thus obtain the following calculated values, for the thickness and the mobilities of electrons or holes of the samples :

epitaxial layer $w = 0.9$ μm,

$$\mu_n = 250\ [2],\ \mu_p = 90,\ \tau_n = 0.12\ \text{ns},\ \tau_p = 0.3\ \text{ns}$$

epitaxial layer $w = 1.3$ μm,

$$\mu_n = 250\ [2],\ \mu_p = 48,\ \tau_n = 0.26\ \text{ns},\ \tau_p = 1.3\ \text{ns}$$

epitaxial layer $w = 2.4$ μm,

$$\mu_n = 250\ [2],\ \mu_p = 80,\ \tau_n = 0.90\ \text{ns},\ \tau_p = 3\ \text{ns}\ .$$

The above values $\tau_{n,p}$ used in expression $\Delta n, p = G\tau_{n,p}$ give the order of magnitude of the densities $\Delta n, p$ which are involved in the present studies, depending on the incident light pulse energie $E_0$. For the case of 1.06 μm light pulses where $G$ is estimated from the intensity $E_0$ (mJ) incident on the sample for a surface reflection of 20 % and an absorption coefficient $\alpha = 40\ \text{cm}^{-1}$, we obtain :

$$W = 0.9\ \mu\text{m}\ (p_0 = 5 \times 10^{16}\ \text{cm}^{-3}),$$
$$\Delta n\ (\text{cm}^{-3}) = 2.5 \times 10^{15} \times E_0\ (\text{mJ}),$$
$$\Delta p\ (\text{cm}^{-3}) = 6 \times 10^{15} \times E_0\ (\text{mJ}).$$
$$W = 1.3\ \mu\text{m}\ (p_0 = 7.5 \times 10^{16}),$$
$$\Delta n\ (\text{cm}^{-3}) = 5 \times 10^{15} \times E_0\ (\text{mJ}),$$
$$\Delta p\ (\text{cm}^{-3}) = 5 \times 10^{16} \times E_0\ (\text{mJ}).$$
$$W = 2.4\ \mu\text{m}\ (p_0 = 3.6 \times 10^{16}\ \text{cm}^{-3}),$$
$$\Delta n\ (\text{cm}^{-3}) = 1.8 \times 10^{16} \times E_0\ (\text{mJ}),$$
$$\Delta p\ (\text{cm}^{-3}) = 6 \times 10^{16} \times E_0\ (\text{mJ}).$$

Since the incident energy used $E_0$ (1.06 μm) varied between $\sim 10^{-4}$ mJ and $10^2$ mJ, the measurements done at ambient temperature with 1.06 μm light correspond to the following range of excess electron or hole densities, where low to high injection rates $\Delta n, p/p_0$ thus appear involved :

epitaxial layer $w = 0.9$ μm

$$\frac{\Delta n}{p_0} = 4 \times 10^{-6} \text{ to } 4,\quad \frac{\Delta p}{p_0} = 10^{-5} \text{ to } 10$$

epitaxial layer $w = 1.3$ μm

$$\frac{\Delta n}{p_0} = 10^{-5} \text{ to } 10,\quad \frac{\Delta p}{p_0} = 10^{-4} \text{ to } 10^2$$

epitaxial layer $w = 2.4$ μm

$$\frac{\Delta n}{p_0} = 5 \times 10^{-5} \text{ to } 50, \quad \frac{\Delta p}{p_0} = 2 \times 10^{-4} \text{ to } 2 \times 10^{2}$$

4.2 ANALYTICAL DESCRIPTION OF TRANSIENT PHOTORESPONSE RESULTS. — We recall first that, for the three cases of transient photoresponses that are used in the present work, the responses given by the epitaxial samples must be considered *a priori* as the sum of two contributions : a *primary* contribution which agree with a contribution of excess free carriers, and a *secondary* contribution which appears as a perturbation of the electrical state of the material following the injection of these free carriers, e.g., perturbation of the electronic occupation state $n_E$, $p_E$ of energy levels $E$ located in the bandgap, and therefore of the charge carrier density, $p(p_0, \Delta p, \sum n_D, \sum p_A)$, mobility, $\mu(p_0 + \Delta n, p)$, in the material, etc... [4].

4.2.1 *Constant current photoconductivity* $\Delta V_\sigma(t)$. — Under constant current $I_0$ the transient photoconductivity response $\Delta V_\sigma(t)$ is given by :

$$\Delta V_\sigma(t) = \frac{I_0 \, l}{we}\left[\frac{1}{\sigma_{tot}(t)} - \frac{1}{\sigma_0}\right] \tag{4}$$

where $\sigma_0$ is the equilibrium conductivity of the material (P-type).

$$\sigma_0 = q p_0 \, \mu p_0 \tag{5}$$

and $\sigma_{tot}$ the conductivity induced in the lighted volume $l \times w \times e$ of the sample (sample width $e = 5$ mm).

$\sigma_{tot}$ may be expressed as follows, taking into account the role played by the free excess carrier $\Delta n, p(t)$ and the variations in the localized charge states $n_E$, $p_A$, respectively [4] :

$$\sigma_{tot}(t) = \sigma_{eff}(t) + \Delta\sigma_{eff}(t)$$

with (6)

$$\sigma_{eff}(t) = q p_{eff}(t) \, \mu_{p\,eff}(t)$$
$$\Delta\sigma_{eff}(t) = q[\Delta p(t) \, \mu_{p\,eff}(t) + \Delta n(t) \, \mu_{n\,eff}(t)] .$$

Considering the general case where the localized charge states refer to point defects as well as to *extended defects* surrounded by potential barrier $\varphi_B$, and assuming that the zones with surrounding potential barrier $\varphi_B$ lead to insulating regions (i.e., internal hole density $p_{jo}$ small compared with the bulk charge carrier density $p_{ov}$ in P-type material), the expressions for $p_{eff}$ and $\mu_{n,p\,eff}$ in (4) have the following forms [5, 6, 17] :

(1) for the charge carrier density ([3])

$$p_{eff} = [p_{ov} + \sum n_D - \sum p_A][1 - f(\varphi_B)] \tag{7}$$

where the first term describes the contribution of the *point defects* to the effective bulk hole density, and the second term the influence of the potential barrier regions $\varphi_B$ on the effective density of the charge carriers $p_{eff}$ ;

and (2) for the carrier mobilities :

$$\mu_{p\,eff} = \frac{\mu_{pv}(\Delta p)}{(1 + f(\varphi_B)/2)}, \quad \mu_{n\,eff} = \frac{\mu_{nv}(\Delta n)}{(1 - f(\varphi_B))^2} \tag{8}$$

where $\mu_{n,pv}$ is the bulk electron or hole mobility taking into account the ionized scattering centers created by the carrier excitation. The terms $(1 + f(\varphi_B)/2)$ and $(1 - f(\varphi_B))^2$ in (8) come from the opposite effects of the insulating regions on the majority and minority carriers, respectively.

In expressions (7) and (8) $f(\varphi_B)$ is the fraction of the material volume which is occupied by the insulating regions with potential barrier $\varphi_B$. In the case of spherical insulating regions with radius $r$ and density $N_j$, the expression for $f(\varphi_B)$ is :

$$f(\varphi_B) = N_j \times \tfrac{4}{3}\pi r^3 \tag{9}$$

in which using the Poisson equation, $r \propto (\varphi_B/p_v)^{1/2}$, the variation of $f$ with $\varphi_B$ thus obeys the following relation :

$$f(\varphi_B) = B(\varphi_B/p_v)^{3/2} \tag{10}$$

where $B$ is a constant.

From the above expressions (5) to (10), the photoconductivity responses may thus be separated into a term, $\Delta V_{\sigma l}(t)$, which depends on the free excess carriers $\Delta p$, $n(t)$, and a term related to the perturbations $p_{eff}(t)$ $\mu_{p,n\,eff}(t)$ in the material which follow the creation of this excess of charge carriers, $\Delta V_{\sigma\,mat}(t)$ :

$$\Delta V_\sigma(t) = \Delta V_{\sigma l}(t) + \Delta V_{\sigma\,mat}(t) \tag{11}$$

so that :

$$\Delta V_{\sigma l}(t) = \frac{I_0 \, l}{we}\left[-\frac{\Delta_{\sigma eff}(t)}{\sigma_{eff}(t)\,(\sigma_{eff}(t) + \Delta\sigma_{eff}(t))}\right]$$
$$\Delta V_{\sigma\,mat}(t) = \frac{I_0 \, l}{we}\left[\frac{1}{\sigma_{eff}(t)} - \frac{1}{\sigma_0}\right]. \tag{12}$$

4.2.2. *Short-circuit photocurrent.* — The expression for the short-circuit photocurrent may also be decomposed into two terms corresponding to the contribution from the free excess carriers collected $i_{hv}(t)$ and to the component $i_j(V_j)$ induced as a result of that excess into the material [13] :

$$i(t) = i_{hv}(t) + i_j(V_j) . \tag{13}$$

The excitation pulse $g(t)$ is triangular, with a width at half maximum $\delta/2 = 30$ ns. Since the free carrier

([3]) The effective minority carrier density is given by [17]

$$n_{eff} = n_v[1 - f(\varphi_B)] .$$

lifetimes $\tau_{n,p} < 3$ ns are small compared to the pulse duration, the component related to free carriers obeys the relation :

$$i_{hv}(t) = i_0(t) + i_{Dn,p}(t) \tag{14}$$

where

$$i_0(t) = qAw_t\, g(t) \tag{15}$$

is the conduction photocurrent due to the electron-hole pairs created within the depleted region $w_t$ of the $N^+$, $P^+/P$ transition (area $A$), and :

$$i_{Dn,p}(t) \simeq qAL_{n,p}\, g(t) \tag{16}$$

is the diffusion photocurrent due to the free excess electrons or holes in the P layer.

The free carrier component $i_{hv}(t)$ thus follows the light excitation pulse $g(t)$.

The term which depends on the evolution of the transition regions is related to the behaviour of the voltage $V_j$ associated with the collection zone under the effect of carrier injection. In the present results, where comparable slow component $i_2$ appear in the $i(PP^+)$ and $i(PN^+)$ photocurrent signals (see § 3.2) the $i_j(V_j)$ term may be written in the form (see appendix) :

$$i_j(v_j) = C_j(t)\frac{1-K}{q}\frac{dE_F(t)}{dt} \tag{17}$$

where $E_F(t)$ is the hole Fermi level $E_F(p_{eff})$ of the silicon layer and $C_j \propto V_j^{-K}$ the capacity of the collecting zone. Thus the $i_j(V_j)$ contribution should reflect the variations of the material Fermi level.

4.3 ANALYSIS OF THE OBSERVED PHOTORESPONSES. — 4.3.1 *Short circuit photocurrents* — From expressions (13) to (17) above, the prompt components $i_1(t)$ of the $i_n(t)$ and $i_p(t)$ measured responses agree with the free electron and hole currents $i_{hv}(t)$.

On the other hand, the negative slow components $i_2(t > \delta)$ also agree with the evolution of the collecting zones $i_j(V_j)$ as described by expression (17). This gives :

$$i_j(V_j) < 0 \tag{18}$$

and thus from (17)

$$\frac{dE_F}{dt} < 0\,. \tag{19}$$

Therefore, the material Fermi level $E_F$ appears to be decreased with respect to its initial value $E_{Fo}$. This indicate an increase in the density $p_{eff}$ of conduction carriers in the material of initial density $p_0$, especially at the times $t > \delta$ where the free excess carriers $\Delta n$, $p(t)$ have disappeared.

4.3.2 *Conductivity photoresponses* $\Delta V_\sigma(t)$. — On the same way, in order to understand the behaviour of the amplitudes and the forms of the signals observed, the contribution $\Delta V_{\sigma\,mat}$ of the material must be considered, as was the case for the short circuit photocurrent responses. Indeed, from the studies of constant current photoconductivity, we find that :

1) No noticeable primary contribution of free carriers, electrons and holes, is observed in the photoconductivity photoresponses ([4]) (i.e. $\Delta V_{\sigma i}(t < \delta) \sim 0$ in expression (12)).

2) Only a delayed perturbation induced in the effective conductivity of the material may correspond to the photoconductivity responses $\Delta V_\sigma(t)$ measured for times $t > \delta$, after the excitation pulse.

3) Moreover, whatever the samples and their thicknesses, the responses $\Delta V_\sigma(t > \delta)$ observed have the characteristics expected for $\Delta V_{\sigma\,mat}(t)$ : they show an exponential type growth which agrees with the carrier filling of traps; then, they have a very slow decrease whose time constant $\tau_\sigma(t)$ increases with time and which is thus typical of the reemission of trapped carriers where associated with the restoration of a surrounding potential barrier [1, 18].

4) Furthermore, the signals $\Delta V_\sigma(t) \sim \Delta V_{\sigma\,mat}(t)$ always correspond to an increase in the effective conductivity of the sample (see Fig. 10), and this conductivity rise compares well with the behaviour of the slow photocurrent $i_2(t)$ (see expressions (6), (12) and (18), (19)).

In summary, it appears that :

(1) The transient current and conductivity photoresponse results are in agreement with the presence of zones having an insulating influence : insulating zone are surrounded by potential barriers whose effect — i.e., decrease of the equilibrium mobility and the effective density of the conduction holes in bulk silicon at equilibrium compared with hole mobility and density (see expressions (7) and (8)) — is decreased or even suppressed by the injected carriers. In the case of silicon epitaxial layers, such zones have been explained as clusters of defects [1, 18] which capture the free carriers and, as a consequence, the potential barriers $\varphi_B$ surrounding them are decreased; therefore, the limiting effects of these zones on the material conductivity $\sigma = qp(\varphi_B)\,\mu_p(\varphi_B)$ are decreased. Note that in the present work, photoexcitation especially appears to induce an increase in the effective hole density $p_{eff}(t) = p(\varphi_B)$ with $\varphi_B(t)$, in agreement with the expressions (7) and (8) for insulating regions.

(2) It is the zones of potential barrier having an insulating behaviour which control the photoconduction of the silicon on sapphire samples studied.

([4]) The rapid parasite response associated with the open circuit response $v_{oc}$ may eliminate the component $\Delta V_{\sigma i}$ associated with free carriers in the signals $\Delta V_\sigma$ measured.

Therefore :

First, in view of the insulating character of these zones, the trapped carriers will be the minority carriers (in this case, electrons). The trapping levels determined by the measurements of photoconductivity as a function of temperature must be electron traps with levels

$$E_c - E_t = 0.14\ \text{eV} \pm 0.03\ \text{eV}$$
(epitaxial layer $w = 0.9\ \mu\text{m}$)

$$E_c - E_t = 0.17\ \text{eV} \pm 0.07\ \text{eV}$$
(epitaxial layer $w = 2.4\ \mu\text{m}$) .

Second, both the minority carrier capture (which induces changes in the electronic charge states $n_{Ej}$ of the energy levels located inside the insulating region) and the internal generation of excess electron-hole pairs $\Delta n_j$, $p_j$ are involved in the decrease of the potential barrier from its initial value $\varphi_{B0}$ to a lower value $\varphi_B = \varphi_{B0} - \Delta\varphi_B$ such as :

$$\begin{aligned} \varphi_{B0} &= kT\,\text{Log}\,(p_{0v}/p_{j0}) \\ \varphi_B(t) &= kT\,\text{Log}\,(p_v/p_j) \\ \Delta\varphi_B(t) &= kT\,\text{Log}\,(p_j/p_{j0} \times p_{0v}/p_v) \end{aligned} \tag{20}$$

where

$$\begin{aligned} p_v &= p_{0v} + \Delta p \\ p_j &= p_{j0} + \Delta p_j + \sum n_{Dj} . \end{aligned} \tag{21}$$

Now, we must remark that, for all epitaxials, our results show that starting at injection level

$$\Delta p/p_0 \sim 10^{-3}$$

the values of $\tau_{\sigma 1,2}(\Delta p/p_0)$ stabilize and the amplitude $\Delta V_{\sigma\,max}(\Delta/p_0)$ becomes a sub-linear function of $\Delta/p_0$. Thus, at $\Delta p/p_0 \sim 10^{-3}$ the excess carrier density $(p_j - p_{j0})$ induced in the insulating regions is large enough to give a notable decrease $\Delta\varphi_B$ of the barrier height $\varphi_B$, i.e. (cf. (20), (21)) :

$$\Delta\varphi_B = kT\,\text{Log}\left(1 + \frac{\Delta p_j + \sum n_{Dj}}{p_{j0}}\right) \tag{22}$$

with

$$\Delta p_j + \sum n_{Dj} \sim p_{j0} .$$

As it is the conditions $\Delta p_j < \Delta p$ and $\sum n_{Dj} > \Delta n$ are satisfied inside the insulating regions, we can assume that a notable decrease $\Delta\varphi_B$ roughly corresponds to the following inner carrier injection :

$$\Delta p_j + \sum n_{Dj} \sim p_{j0} \sim \Delta p .$$

The equilibrium Fermi level $E_{Fj}$ associated with these insulating regions therefore corresponds to

$$E_{Fj} \simeq E_v + 0.32\ \text{eV}$$

and the potential barriers $\varphi_{B0}$ to : $\varphi_{B0} = E_{Fj} - E_{FV}$

epitaxial layer $w = 0.9\ \mu\text{m}$

$$\varphi_{B0} \sim 0.19\ \text{eV}$$

epitaxial layer $w = 1.3\ \mu\text{m}$

$$\varphi_{B0} \sim 0.17\ \text{eV}$$

epitaxial layer $w = 2.4\ \mu\text{m}$

$$\varphi_{B0} \sim 0.15\ \text{eV} .$$

(3) Finally, it is also to be noticed that, when $\Delta n$, $p$ increases to values of high injection $\Delta n$, $p > p_0$, the amplitude of the responses $\Delta V_{\sigma\,mat}$ takes on a saturation value. This value then remains well below the applied equilibrium voltage $V_e(\sigma_0, I_0)$ of the illuminated zone. Thus, with the potential difference $V_e - \Delta V_{sat}$ which governs the illuminated zone, there is associated an effective conductivity for the material $\sigma_{eff\,sat} > \sigma_0$ which corresponds to the *transient disappearance* of insulating zones under the effect of the injection. The *constraint* on the conductivity given by the insulating regions may then be estimated by the variation of the conductivity $\sigma_{eff\,sat} - \sigma_0$. For each of the epitaxial samples studied, the values are :

0.9 μm sample ($\sigma_0 = 1.47\ \Omega^{-1}\ \text{cm}^{-1}$),

$$\sigma_{eff\,sat} = 1.84 , \quad (\sigma_{eff\,sat} - \sigma_0)/\sigma_0 = 25\ \%$$

1.3 μm sample ($\sigma_0 = 0.63\ \Omega^{-1}\ \text{cm}^{-1}$),

$$\sigma_{eff\,sat} = 0.84 , \quad (\sigma_{eff\,sat} - \sigma_0)/\sigma_0 = 33\ \%$$

2.4 μm sample ($\sigma_0 = 0.50\ \Omega^{-1}\ \text{cm}^{-1}$),

$$\sigma_{eff\,sat} = 0.67 , \quad (\sigma_{eff\,sat} - \sigma_0)/\sigma_0 = 34\ \% .$$

Taking into account the increase in $\sigma_0$ due to $P^+$ zones in the sample of thickness $w = 0.9\ \mu\text{m}$ due to an accidental supplementary diffusion during the implantation of the contacts, the above results show that the contribution of the insulating zones represents a constant factor for the three series of LETI epitaxials studied.

5. **Conclusion.** — This study has been concerned with the epitaxial layer conduction parameters from their average values over the layer thickness. We have obtained results on the respective contributions of free carriers and zones of electrical inhomogeneity in samples of silicon on sapphire.

The Hall data indicated the presence of donor-type compensation levels and the influence of ionized impurities and dislocations on the conduction carriers. These results compare well with the transient photoresponse (especially photoconductivity $\Delta V_\sigma(t)$) results which clearly show that strong effects coming from electrical inhomogeneities are involved in the electrical properties of the layers studied.

Concerning the electrical characterization of these layers the results of the paper, while giving only an approximate evaluation of the parameters, allow us :

1) to set off the existence of zones having an insulating behaviour with $E_{Fj} \simeq E_V + 0.32$ eV, and $\varphi_{B0} \simeq 0.17$ eV for a layer of resistivity $\sim 1.5\,\Omega.\text{cm}$;

2) to show that electron traps

$$E_t \sim E_c - 0.17\text{ eV} \pm 0.07\text{ eV}$$

are involved;

3) to evaluate the decrease in the layer conductivity which is associated with *insulating zones* — 33 % in the layers studied here whatever the sample thickness is;

4) to observe that the zones having insulating behaviour thus appear to spread out in the layer volume and not to remain localized at the interface.

Note that the results (1) and (2) are in agreement with those obtained by other authors [1, 19] in S.O.S. materials.

**Appendix.** — The short circuit photocurrent may be decomposed into two terms :

$$i(t) = i_{h\nu}(t) + i_j(V_j) \qquad \text{(A 1)}$$

where $i_j(V_j)$ is the term related to the evolution of the collecting zone under the influence of the injection of carriers. It is related to the evolution of the voltage $V_j$ associated with the collecting zone under the influence of carrier injection. Assuming a collecting zone with equilibrium diffusion voltage $V_D$ and with capacity $C_j$ in the form $C_j \propto V_j^{-K}$, the $i_j$ term may be expressed by :

$$i_j(V_j) = \frac{dQ_j}{dt} = C_j(t)\,(1 - K)\,\frac{dV_j}{dt} \qquad \text{(A 2)}$$

where

$$V_j(t) = V_D + \Delta V_j(t)\,. \qquad \text{(A 3)}$$

For the case of $PN^+$ junction, we have

$$qV_{Dn+p} = E_{F0} - E_{Fn+} \qquad \text{(A 4)}$$

while for a $PP^+$ junction,

$$qV_{Dp+p} = E_{F0} - E_{Fp+} \qquad \text{(A 5)}$$

where

$E_{F0}$ is the equilibrium Fermi level in the material,
$E_{Fp+}$ is the equilibrium Fermi level in the $P^+$ zone, and
$E_{Fn+}$ is the equilibrium Fermi level in the $N^+$ zone.

If the hole density is varied in the P type volume of the sample, the induced evolution of the Fermi level from $E_{F0}$ to $E_F(t)$ results in a variation $\Delta V_j(t)$ of the equilibrium value $V_D$ :

$$q\,\Delta V_j(t) = E_F(t) - E_{F0}\,. \qquad \text{(A 6)}$$

Thus, according to the relative values of $E_{F0}$ and $E_F(t)$, we will have either an increase or a decrease of $V_j(t)$ which will in turn influence $i_j(V_j)$ :

$$i_j(V_j) = C_j(t)\,(1 - K)\,\frac{d}{dt}\,\frac{E_F(t) - E_{F0}}{q} \qquad \text{(A 7)}$$

$$i_j(V_j) = C_j(t)\,\frac{(1 - K)}{q}\,\frac{dE_F(t)}{dt}\,. \qquad \text{(A 8)}$$

The $i_j(V_j)$ term given by expression (A 2) then reflects directly the fluctuations of the Fermi level of the P type material.

## References


[1] EERNISSE, E. P., NORRIS, C. B., *Solid State Electron.* **16** (1973) 315.
[2] SCHLÖTTERER, H., *Solid State Electron.* **11** (1968) 947.
[3] GONCHOND, J. P., Thèse Docteur-Ingénieur, Grenoble (1978).
[4] BIELLE-DASPET, D., JOHAN, A., ESPIOUSSAS, F. and ROUX, M., *Revue Phys. Appl.* **15** (1980) 945.
[5] JOHAN, A., AYERZA, J., BIELLE-DASPET, D., ROCHER, A. and FONTAINE, C., 2nd *Photovoltaic Solar En. Conf.*, Berlin (1979).
[6] AYERZA, J., Thèse Docteur-Ingénieur, Toulouse (1980).
[7] GASSET, G., BENZHORA, M., JOHAN, A., BIELLE-DASPET, D., *Revue Phys. Appl.* **14** (1979) 209.
[8] See for instance SZE, S. M., *Physics of semiconductors devices*, (J. Wiley and Son N. Y.) 1970, p. 36.
[9] DUMIN, D. J. and ROSS, E. C., *J. Appl. Phys.* **41** (1970) 3139.
[10] IPRI, A. C., ZEEMEL, J. N., *J. Appl. Phys.* **44** (1973) 744.
[11] LUDWIG, G. W. and WATTERS, R. L., *Phys. Rev.* **101** (1956) 1699.
[12] ABRAHAMS, M. S. and BUIOCCHI, C. B., *Appl. Phys. Lett.* **27** (1975) 325.
[13] BIELLE-DASPET, D., JOHAN, A. and ESPIOUSSAS, F., *Revue Phys. Appl.* **15** (1980) 203.
[14] ROUX, M., Thèse Docteur-Ingénieur, Paris XI (July 1981).
[15] BIELLE-DASPET, D. and GASSET, G., *Solid State Electron.* **21** (1978) 121.
[16] CRISTOLOVEANU, S., CHOVET, A. and KAMARINOS, G., *Solid State Electron.* **21** (1978) 1563.
[17] GOSSICK, B. R., Proc. *Intern. Conf. on Semiconductors, Ph. Physics* **20** Prague (1960) 202.
[18] NORRIS, C. B., *Appl. Phys. Lett.* **20** (1972) 187.
[19] DUMIN, D. J., *Solid State Electron.* **13** (1970) 415.
[20] MORIN, F. J., MAITA, J. P., *Phys. Rev.* **96** (1955) 28.